American Journal of Noninvasive Cardiology
Editor-in-Chief: D.H. Spodick, Worcester, MA

Reprint
Publisher: S. Karger AG, Basel
Printed in Switzerland

Am J Noninvas Cardiol 1991;5:343–352

0258–4425/91/0056–0343$2.75/0

Two-Dimensional Echocardiographic Measurements in Systemic Sclerosis and a Matched Reference Population

Elsadig Kazzam[a], *Kenneth Caidahl*[b], *Tomas Gustafsson*[c], *Rolf Gustavsson*[a], *Roger Hällgren*[a], *Johan Landelius*[d], *Anders Waldenström*[a]

Departments of [a] Internal Medicine and [d] Clinical Physiology, University Hospital, Uppsala;
[b] Department of Clinical Physiology, Sahlgren's University Hospital, and [c] Chalmers School of Technology, Gothenburg, Sweden

Key Words. Cardiac dimensions · Echocardiography · Left atrium · Left ventricle · Systemic sclerosis · Right atrium

Abstract. The present study was performed in order to evaluate, by two-dimensional echocardiography, cardiac morphology in terms of chamber dimensions, as well as left ventricular (LV) volume and mass, in patients with systemic sclerosis (n = 30). Measurements were compared with those from age- and sex-matched controls (n = 48). The most prominent finding in patients was increased LV wall thickness. There was also a tendency in patients to have reduced LV cavity dimensions. Thus, interventricular septum ($p < 0.0005$), LV posterior wall ($p < 0.05$) and the wall thickness/cavity dimension ratio ($p < 0.0005$) were increased in patients compared to controls, as was LV mass index ($p < 0.005$). The stroke volume ($p < 0.005$), end-diastolic volume ($p < 0.01$) as well as end-diastolic volume index ($p < 0.05$) were decreased in the patient group, but not when body surface area was considered. Blood pressure, ejection fraction and end-systolic wall stress were similar in the two groups. We conclude that our patients with systemic sclerosis had a nondilated LV cavity, with an increased wall thickness and relative LV mass. LV hypertrophy was not explained by systemic hypertension and may therefore be secondary to myocardial fibrosis.

Introduction

In systemic sclerosis, cardiac involvement seems to be an indicator of poor prognosis [1, 2]. Postmortem studies [3, 4], and M mode echocardiographic evaluation of the present study population [5], have shown that left ventricular (LV) hypertrophy is a common finding in patients with systemic sclerosis. M mode echocardiography has been extensively used for the noninvasive assessment of cardiac dimensions and performance [6–9], and more recently the usefulness of two-dimensional echocardiographic measurements of cardiac dimensions has been demonstrated [10, 11]. The value of two-dimensional echocardiography in the assessment of LV mass [12], volume [13] and stress [14] has been reported.

The aim of the present study was to evaluate cardiac morphology and LV function by two-dimensional echocardiography in patients with systemic sclerosis in comparison with normal controls.

Patients and Methods

Subjects

Thirty consecutive patients (15 men and 15 females; age range 25–77 years, mean 54.5 years), with systemic sclerosis according to the American Rheumatism Association criteria [15] were studied. The patients were referred from Uppsala region to Uppsala University Hospital between December 1986 and March 1988. Their disease had been recognized for 5.6 (range 0.5–23) years. On electrocardiogram none had left bundle branch block, while 1 patient had

Received: June 10, 1990
Revision received: February 1, 1991
Accepted: February 6, 1991

Address for correspondence:
Dr. Elsadig Kazzam, MD
Department of Internal Medicine, Uppsala University Hospital
S-75 185 Uppsala (Sweden)

Table 1. Clinical data of the individual patients with systemic sclerosis (SScl)

No.	Sex age years	Disease duration years	SScl scoring (0–54)	SBP/ DBP mm Hg	TPR dyn (s cm^{-5})	ESR mm/h	FEV_1 % of predicted	Serum creatinine µmol/l	Medication
1	M 68	12	36	140/73	1,452	85	89	72	–
2	M 54	1	29	95/65	2,284	8	73	79	nifedipine
3	M 68	5	34	125/76	1,714	44	45	107	frusemide
4	M 77	0.5	41	125/77	1,832	36	91	97	–
5	F 43	2	30	132/80	1,191	13	51	85	nifedipine
6	F 48	0.5	34	120/75	593	95	72	90	–
7	F 65	7	27	123/73	1,500	8	93	87	–
8	F 67	23	31	127/70	1,126	95	90	68	–
9	F 66	5	25	130/90	2,085	22	76	59	hydrochlorothiazide
10	F 42	0.5	21	165/80	–	20	100	64	verapamil
11	M 59	20	28	122/61	1,358	20	57	79	–
12	F 65	0.5	16	103/64	1,829	22	66	76	–
13	M 59	3	24	127/79	–	7	80	67	–
14	M 50	0.5	8	138/81	1,275	60	56	71	–
15	M 46	4	21	160/70	1,177	56	91	50	–
16	F 70	8	34	157/110	1,393	20	90	79	–
17	M39	1	11	165/80	1,863	8	75	91	digoxin
18	M 48	1	25	125/75	1,306	7	93	80	–
19	F 73	1	37	133/90	920	4	63	78	–
20	M 27	7	10	125/75	2,123	46	121	110	–
21	M 43	10	31	139/88	1,887	10	109	75	–
22	F 51	1	11	110/73	846	18	66	81	–
23	M 63	5	34	145/77	1,298	67	74	72	–
24	M 66	0.5	34	169/66	1,987	54	71	77	–
25	F 25	0.5	8	105/72	2,238	5	70	76	–
26	F 49	1	25	147/87	1,798	50	67	83	frusemide
27	F 47	10	31	118/77	1,095	–	109	–	–
28	M 67	0.6	19	145/92	1,207	40	67	85	–
29	F 41	–	–	125/68	1,426	34	66	67	–
30	F 48	11	–	158/90	2,569	9	81	65	–

F = Female; M = male; SBP = systolic blood pressure; DBP = diastolic blood pressure; TPR = total peripheral resistance; ESR = erythrocyte sedimentation rate; FEV_1 = forced expiratory volume during 1 s as percentage of predicted.

Table 2. General characteristics of the controls and patients (means ± SD)

	Controls n = 48	Patients n = 30	p value
Age, years	54.9 ± 2.1	54.5 ± 2.4	NS
Sex female/male	26/22	15/15	
Height, cm	172.7 ± 1.1	170.9 ± 1.9	NS
Weight, kg	73.1 ± 1.8	65.1 ± 2.0	< 0.05
BSA, m^2	1.9 ± 0.03	1.7 ± 0.04	< 0.05
Systolic blood pressure mm Hg	134.6 ± 2.6	132.9 ± 3.5	NS
Diastolic blood pressure mm Hg	81.6 ± 1.4	78.7 ± 2.1	NS

right bundle branch block. The clinical characteristics and the status of the individual patients are shown in table 1.

For comparative purposes, age- and sex-matched control subjects were selected from the general population of Uppsala. A sample of 90 age- and sex-matched subjects (3 for each patient) was drawn from the population register kept by the County Census Bureau. All controls were informed about the investigation protocol, and 55 of them gave their consent to participate in the study. Controls were excluded if they were treated for hypertension (n = 2), if they had coronary (n = 2) or rheumatic (n = 2) heart disease according to clinical history or electrocardiogram. None of the controls had known renal or pulmonary disease or bundle branch block. One subject was excluded because of inadequate recordings. The remaining 48 subjects (26 men and 22 females, age range 25–77 years, mean 54.6 years) constituted a healthy control group. The general characteristics of the controls and the patients are shown in table 2.

Methods

Two-dimensional echocardiography was performed by means of a Hewlett Packard ultrasound imaging system model 77020A, version K with a 2.5- or 3.5-MHz phased array transducer. The echocardiographic recordings of routine projections, the parasternal long-axis and short-axis (aortic, mitral and papillary) planes and the apical four-chamber, long-axis and two-chamber views were stored on VHS 0.5-inch video tapes by means of a Panasonic video recorder NV 8100.

One investigator (E.K.) carried out all interpretations, and questionable measuring points were agreed upon by consensus with another investigator (K.C.). For the interpretations a special computer program was developed on a minicomputer (LSI-11/23, Digital Equipment Corp.). A framegrabber with 256-kB image memory (Matrox QVAPH + QRGB, 512*152*8), a digitizer (Graphtec KD6040) and a color monitor (VR241, Digital Equipment Corp.) were used. A videosystem with slow-motion and playback facilities (Panasonic) was connected to the computer through the framegrabber, and the recordings were digitized in real time, interpretation being performed in the digitized form. The matrix consisted of 512 lines, 512 pixels (picture elements)/line and 8 bits of gray scale per pixel. The stop frame mode utilized renewed digitization from the next frame (still frame picture) when the video recorder was stopped.

The end-diastolic and end-systolic frames were localized by using the search feature of the tape recorder. End-diastole was defined as the frame at or immediately preceding the R wave of the QRS complex and (when visualized) after atrioventricular valve closure. End-systole was defined by the aortic valve closure, smallest LV cavity dimension or by an immediately following atrioventricular valve opening, as appropriate, in that order. Measurements were performed by manually tracing borders or marking distances with the digitizer or by moving a cursor through the digitized image on the monitor. Tracings and markings were immediately seen on the monitor, and mistakes could easily be corrected. All measurements were performed using the inner (trailing to leading) edge convention. The mean of three beats was used. However, in recordings with only acceptable general quality, the best beat was used if having a better than average quality. Stop frames were excluded if there was more than 10% drop of the endocardium. Distances were not measured if the endocardium was not visible at both ends of the distance, i.e. measuring points were not interpolated from surrounding echoes. We used only projections where the intended orientation was obtained, i.e. e.g. noncircular short-axis images were excluded from measurements. A concave interventricular septum indicating severe pulmonary hypertension was not found. The analyzed dimensions and areas are described in figure 1.

LV mass was calculated according to the formula $1.05 \cdot \pi\ [(b + t)^2(2/3[a + t] + d - d^3/[3(a + t)^2]) - b^2(2/3 \cdot a + d - d^3/[3 \cdot a^2])]$ [12], where a, b, d and t denote the apical part of the long axis and short axis, the basal part of the long axis and the average wall thickness, respectively. From the LV short-axis view at the level of the papillary muscle the total area (muscular + cavity area; A1) and cavity area (A2) were determined, and the myocardial area (Am) was calculated as Am = A1 – A2. Area fractional shortening and fractional shortening were calculated as (diastolic – systlic)/diastolic cavity area and anterioposterior dimension, respectively. The average wall thickness (t) equals the difference between the radii of epicardial (A1) and endocardial (A2) area: $t = \sqrt{A1/\pi} - \sqrt{A2/\pi}$.

Blood pressure was measured in the supine position after 15–30 min of rest. Carotid pulse tracings were used for calculation of end-systolic pressure, assigning diastolic and systolic blood pressure to the nadir and peak of the curve [16]. Only beats with acceptable or good quality were used for measurements. All measurements of the relative height of end-systole compared to total height of the carotid curve were performed by means of a digitizer-computer system (Summagraphics digitizer connected to a PDP 11/34 computer, Digital Equipment). Five beats were measured from pulse curves. The means were used for further calculations. End-systolic wall stress was obtained as 1.33 × end-systolic pressure × A2/Am × 103 dyn/cm^2 [14].

From the apical four-chamber view the end-diastolic and end-systolic volumes were calculated according to the formula volume = 5/6 × area × LV long axis at end-diastole, and ejection fraction was obtained as end-diastolic – end-systolic/end-diastolic volumes. Stroke volume was calculated as ejection fraction × end-diastolic volume.

Lung function was estimated by the measurement of forced expiratory volume in 1 s, the lower normal value in our laboratory being 80% of the predicted value. The erythrocyte sedimentation rate was read after 1 h (Westergren), and serum creatinine was measured at the Department of Clinical Chemistry.

A Raynaud's phenomenon score was based on a 5-grade scale; 0 for no signs of the phenomenon and 4 for the most severe form with cyanotic fingers even at 20 °C.

The severity of skin lesions was assessed by a simple scoring system; skin thickening was estimated at 18 anatomical sites by a 4-grade scale: 0 for normal skin and grade 3 for the most severe thickening and induration of the skin. The maximum score was therefore 54.

Statistics

Measurements are presented as means ± standard deviation. Student's t test was used to evaluate differences between the study groups.

Results

General Characteristics

The general characteristics of the controls and the patients are shown in table 2. In spite of similar heights, patients weighed less than controls. Blood pressure was similar in the two groups.

Interpretability of Two-Dimensional Echocardiography

In the tables the numbers of controls and patients yielding any stop frame measure in the respective view are specified. It seems also pertinent to present the availability for analyses of relevant structures in the motion mode and the number of investigations allowing all attempted measurements in stop frame mode.

Out of the 30 patients/48 controls the motion mode (and all measures in the stop frame mode) were available

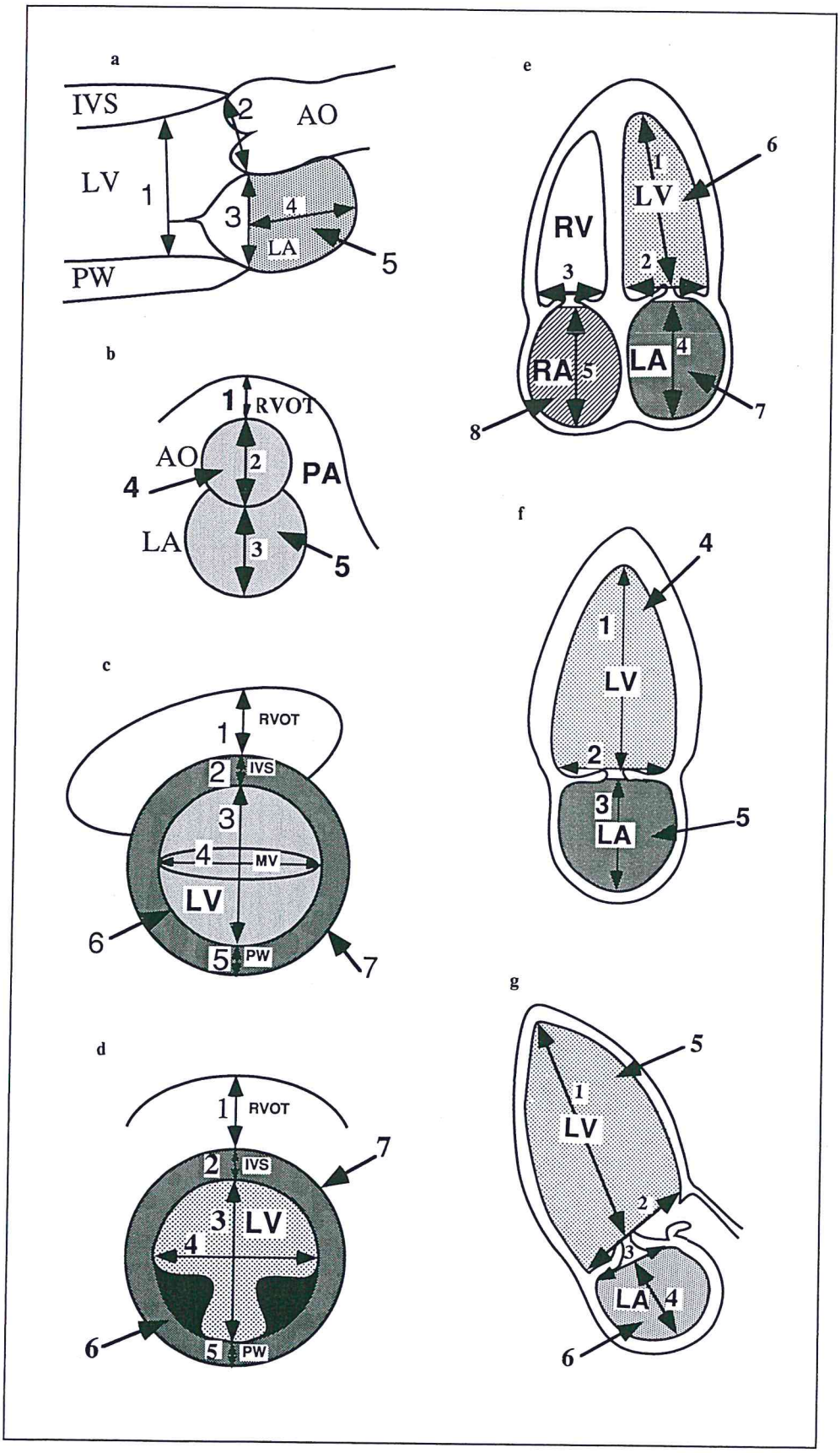

Fig. 1. Measurements of dimensions. In addition to the marked dimensions, the LV area was measured in the apical views, the left atrium in the apical long-axis view and both atria in the four-chamber view. AO = Aorta; IVS = interventricular septum; LA = left atrium; LV = left ventricle; MV = mitral valve; PA = pulmonary artery; PM = papillary muscle; PW = posterior wall; RA = right atrium; RV = right ventricle; RVOT = right ventricular outflow tract.

a Parasternal long-axis view. 1 = LV mid cavity (mitral tip); 2 = AO diameter; 3 = mitral orifice; 4 = LA long-axis diameter; 5 = LA area.

b Parasternal short-axis view: AO level. 1 = RVOT; 2 = AO anterioposterior diameter; 3 = LA anterioposterior diameter; 4 = AO area; 5 = LA urea.

c Parasternal short-axis view: MV level. 1 = RVOT; 2 = septal thickness; 3 = LV anterioposterior diameter; 4 = LV mid cavity diameter; 5 = PW thickness; 6 = LV cavity area; 7 = LV cavity + myocardial area.

d Parasternal short-axis view: PM level. 1 = RVOT; 2 = septal thickness; 3 = LV anterioposterior diameter; 4 = LV mid cavity diameter; 5 = PW thickness; 6 = LV cavity area; 7 = LV cavity + myocardial area.

e Apical four-chamber view. 1 = LV long axis; 2 = LV base; 3 = RV base; 4 = LA long axis; 5 = RA long axis; 6 = LV area; 7 = LA area; 8 = RA area.

f Apical two-chamber view. 1 = LV long axis; 2 = LV base; 3 = LA long axis; 4 = LV area; 5 = LA area.

g Apical long-axis view. 1 = LV long axis; 2 = LV base; 3 = mitral orifice; 4 = LA long axis; 5 = LV area; 6 = LA area.

Table 3. Left parasternal long-axis view (means ± SD)

		Uncorrected			Adjusted for BSA (/m²)		
		controls n = 43	patients n = 28	p	controls n = 43	patients n = 28	p
Aortic diameter, mm	D	20±2.9	21±3.7	NS	11.1±1.4	12.1±1.8	<0.05
	S	22±3.0	23±3.7	NS	11.8±1.5	13.2±2.2	<0.005
LA mitral orifice, mm	D	23±3.5	25±4.5	NS	12.7±2.0	14.4±2.8	<0.05
	S	33±4.3	34±4.2	NS	18.1±2.4	19.6±3.2	<0.05
LA diameter long-axis, mm	D	31±5.1	35±8.2	<0.05	17.3±2.9	20.4±4.9	<0.005
	S	45±7.1	45±8.3	NS	24.3±4.0	26.5±7.4	NS
LA area, mm²	D	594±184	717±306	<0.05	323±94	416±170	<0.005
	S	1,189±283	1,213±426	NS	647±149	711±282	NS
LV diameter mid cavity, mm	D	47±4.8	48±7.3	NS	25.6±2.8	27.6±4.4	<0.05
	S	35±6.9	36±8.7	NS	19.2±3	20.1±4.6	NS

D = End-diastole; S = end-systole; LA = left atrial; LV = left ventricular.

in the following numbers: parasternal long-axis view 28 (28)/44 (44); parasternal short-axis projection (aortic view) 20 (13)/46 (34); parasternal short-axis (mitral) view 22 (10)/47 (29); parasternal short-axis (papillary) view 22 (11)/46 (28); four-chamber view 27 (23)/47 (46); apical long-axis view 24 (20)/45 (43), and apical two-chamber view 24 (21)/40 (39).

To evaluate the relation between the image quality and age, height, weight, body surface area (BSA) and body mass index, we correlated these variables with picture quality. We found significant correlations between image quality in all views (both motion and stop frame pictures) and age. The quality of apical recordings (motion as well as stop frame) was also significantly correlated to the body mass index.

Dimensions

Dimensional data for each echocardiographic view are presented in tables 3–9. Noncorrected values are shown on the left, and measurements adjusted for BSA are displayed on the right. Since patients had lower BSA than controls, measures having similar values in the uncorrected form gave increased values for patients after adjustment for BSA, while low values among patients turned out to be normal after adjustment for BSA.

The aortic diameter did not differ between patients and controls (tables 3, 4), although after adjustment for BSA patients had a 1 mm larger diameter than controls in the parasternal long-axis view.

The left atrium tended to be larger in patients, but not in all views (tables 3, 4, 7–9). After adjustment for BSA the left atrium was markedly longer, and its systolic area increased in the apical four-chamber view, compared to the left atrium in controls (table 7).

The left ventricle was smaller in patients as judged from apical projections (tables 7–9), but this was not the case when body size was taken into account.

Neither the right atrium (table 7) nor the right ventricle (tables 4–7) were increased among patients. This fact was not influenced by considerations of body size.

The LV myocardial thickness was increased in diastole, whether measured as septal or posterior wall thickness (tables 5, 6). There was a tendency to increased LV wall area, and this measure was clearly abnormal in the parasternal short-axis view at the papillary level when BSA was considered (table 6). Combined measures of LV hypertrophy (table 10) revealed increased LV wall thickness, thickness/cavity ratio as well as LV mass index.

LV Systolic Function

Ejection fraction, fractional area change and end-systolic wall stress were similar in the two groups (table 11). For the patients and controls considered together, calculations of end-systolic wall stress from two-dimensional echocardiography yielded higher values than those previously found from M mode (68.5 ± 2.9 vs. 58.6 ± $1.9 \cdot 10^3$ dyn/cm², $p < 0.005$). Stroke volume was decreased in the patients.

Table 4. Left parasternal short-axis view: aortic level (means ± SD)

		Uncorrected			Adjusted for BSA (/m²)		
		controls n = 43	patients n = 28	p	controls n = 43	patients n = 28	p
Aortic AP diameter, mm	D	25±3.5	25±6.5	NS	14±1.5	14±2.7	NS
	S	29±5.4	29±6.3	NS	15±2.3	16±3.0	NS
Aortic area, mm²	D	489±138	534±223	NS	263±74	298±97	NS
	S	624±178	667±291	NS	335±82	380±128	NS
LAAP diameter, mm	D	26±5.1	28±5.8	NS	14±3.0	16±3.2	NS
	S	32±5.7	33±6.9	NS	17±2.9	19±3.3	NS
LA area, mm²	D	840±333	884±230	NS	456±182	512±146	NS
	S	1,264±348	1,305±400	NS	680±167	750±214	NS
RV outflow tract, mm	D	35±6.3	32±5.9	NS	19±2.7	19±5.8	NS
	S	28±5.8	24±5.5	NS	15±3.0	14±5.1	NS

D = End-diastole; S = end-systole; RV = right ventricular; AP = anterioposterior; LA = left atrial.

Table 5. Left parasternal short-axis view: mitral valve level (means ± SD)

		Uncorrected			Adjusted for BSA (/m²)		
		controls n = 43	patients n = 28	p	controls n = 43	patients n = 28	p
IVS thickness, mm	D	9.8±1.5	12.3±2.2	<0.0005	5.4±0.7	7.1±1.6	<0.0005
	S	12.2±1.7	13.0±2.6	NS	6.7±0.9	7.5±1.9	NS
PW thickness, mm	D	8.4±1.5	10.9±2.0	<0.0005	4.6±0.8	6.4±2.3	<0.0005
	S	11.0±2.3	12.8±3.8	NS	6.1±1.1	7.5±2.9	<0.05
LV wall area, mm²	D	3,469±743	3,739±846	NS	1,884±325	2,157±581	NS
	S	2,767±527	3,245±717	<0.05	1,515±225	1,864±460	<0.005
LV AP diameter, mm	D	49±5.4	48±7.7	NS	27±2.9	28±4.8	NS
	S	36±5.1	37±9.8	NS	20±2.9	21±6.4	NS
LV mid cavity, mm	D	44±5.6	44±6.4	NS	24±3.2	26±6.9	NS
	S	32±5.7	34±3.4	NS	18±3.4	20±4.2	NS
LV area, mm²	D	1,807±427	17,990±385	NS	988±220	1,023±180	NS
	S	1,115±597	1,079±667	NS	621±372	613±122	NS
RV outflow tract, mm	D	28±11	25±6.8	NS	15±7.3	15±4.4	NS
	S	26±6.1	26±6.5	NS	14±3.1	15±3.6	NS

D = End-diastole; S = end-systole; RV = right ventricular; IVS = interventricular septum; PW = posterior wall; AP = anterioposterior.

Table 6. Left parasternal short-axis view: papillary muscle level (means ± SD)

		Uncorrected			Adjusted for BSA (/m²)		
		controls n = 43	patients n = 28	p	controls n = 43	patients n = 28	p
IVS thickness, mm	D	9.5±1.4	12.6±1.8	<0.0005	5.2±0.7	7.4±2.1	<0.0005
	S	12.2±2.4	14.8±3.1	<0.05	6.7±1.2	8.6±2.3	<0.0005
PW thickness, mm	D	9.1±1.6	10.7±2.5	<0.05	5.0±1.0	6.2±2.2	<0.05
	S	11.2±2.2	14.7±2.9	<0.0005	6.2±1.2	8.5±2.3	<0.0005
LV wall area, mm²	D	3,451±461	3,967±561	<0.05	1,880±193	2,300±461	<0.0005
	S	2,677±403	3,219±762	<0.05	1,470±214	1,865±510	<0.005
LV AP diameter, mm	D	49±4.9	51±6.0	NS	27±2.5	29±5.7	NS
	S	37±9.2	36±6.8	NS	20±6.2	21±4.9	NS
LV mid cavity, mm	D	43±4.9	43±4.9	NS	24±3.0	25±7.2	NS
	S	28.7±4.8	30.8±4.4	NS	16±2.8	18±5.0	NS
LV area, mm²	D	1,707±288	1,781±305	NS	931±144	1,021±199	NS
	S	855±217	928±280	NS	472±133	531±163	NS
RV outflow tract, mm	D	23±6.2	21±6.8	NS	13±3.1	12±6.2	NS
	S	26±6.1	26±7.1	NS	14±3.2	14±5.7	NS

D = End-diastole; S = end-systole; RV = right ventricular; IVS = interventricular septum; PW = posterior wall.

Table 7. Apical four-chamber view (means ± SD)

		Uncorrected			Adjusted for BSA (/m²)		
		controls n = 43	patients n = 28	p	controls n = 43	patients n = 28	p
LA long-axis diameter, mm	D	37±7.0	44±9.9	<0.01	20±3.6	25±5.4	<0.0005
	S	49±6.8	52±8.2	NS	27±4.2	30±4.9	<0.005
LA area, mm²	D	933±801	1,068±329	NS	513±501	620±199	NS
	S	1,382±330	1,580±384	<0.05	613±214	748±167	<0.005
RA long-axis diameter, mm	D	40±7.3	42±8.7	NS	22±3.8	24±4.7	<0.05
	S	50±5.8	51±7.8	NS	27±3.4	30±4.7	<0.05
RA area, mm²	D	1,141±306	1,241±388	NS	615±159	719±213	<0.05
	S	1,652±334	1,664±390	NS	892±171	967±207	NS
LV long-axis diameter, mm	D	80±9.2	73±9.6	<0.01	43±4.7	43±5.0	NS
	S	66±9.9	63±9.2	NS	36±4.6	36±4.9	NS
LV base diameter, mm	D	44±5.1	44±6.1	NS	24±2.5	25±3.2	<0.05
	S	36±6.2	35±7.9	NS	20±3.1	20±4.0	NS
LV area, mm²	D	3,140±668	2,720±596	<0.05	1,960±268	1,566±289	NS
	S	2,010±551	1,713±469	<0.05	1,079±251	982±235	NS
RV base diameter, mm	D	38±4.6	36±7.0	NS	21±2.7	21±3.5	NS
	S	31±4.2	31±5.8	NS	17±2.4	18±2.8	NS

D = End-diastole; S = end-systole; RV = right ventricular; RA = right atrial; LA = left atrial.

Table 8. Apical long-axis view (means ± SD)

		Uncorrected			Adjusted for BSA (/m²)		
		controls n = 43	patients n = 28	p	controls n = 43	patients n = 28	p
LA mitral orifice, mm	D	27±3.8	26±4.8	NS	14±1.8	15±3.3	NS
	S	32±6.1	31±5.2	NS	17±3.2	18±3.2	NS
LA long-axis diameter, mm	D	43±7.0	46±9.9	NS	24±4.3	27±6.0	<0.05
	S	55±6.2	54±7.7	NS	30±4.5	32±6.0	NS
LA area, mm²	D	890±253	1,007±340	NS	481±126	587±186	<0.05
	S	1,516±335	1,650±464	NS	821±174	961±266	<0.05
LV long-axis diameter, mm	D	75±9.7	71±9.8	NS	41±5.3	42±5.3	NS
	S	62±9.7	60±8.1	NS	34±5.0	36±5.9	NS
LV base diameter, mm	D	46±5.3	44±6.6	NS	25±2.6	26±4.4	NS
	S	37±6.6	36±10	NS	20±3.3	21±6.4	NS
LV area, mm²	D	2,831±511	2,425±604	<0.05	1,529±244	1,415±288	NS
	S	1,835±501	1,454±414	<0.005	989±245	853±232	<0.05

D = End-diastole; S = end-systole; RV = right ventricular; RA = right atrial; LA = left atrial.

Table 9. Apical two-chamber view (means ± SD)

		Uncorrected			Adjusted for BSA (/m²)		
		controls n = 43	patients n = 28	p	controls n = 43	patients n = 28	p
long-axis diameter, mm	D	43±8.3	42±8.4	NS	23±4.7	25±5.8	NS
	S	55±8.3	51±8.6	NS	30±5.0	31±607	NS
LA area, mm²	D	1,116±262	1,234±387	NS	600±155	739±250	<0.05
	S	1,784±319	1,753±396	NS	958±185	1,056±311	NS
LV long-axis diameter, mm	D	77±8.3	71±8.9	<0.05	41±5.1	43±8.4	NS
	S	64±9.1	60±8.2	NS	35±5.3	36±7.1	NS
LV base diameter, mm	D	45±5.2	41±7.5	<0.05	24±3.0	25±6.4	NS
	S	35±6.1	30±6.1	<0.005	19±3.6	18±3.9	NS
LV area, mm²	D	2,934±541	2,398±431	<0.0005	1,568±262	1,444±355	NS
	S	1,818±493	1,479±417	<0.05	971±243	880±242	NS

D = End-diastole; S = end-systole; LA = left atrial.

Control Group Compared to Previously Published Data from Normals

In table 12 some measurements from the controls are displayed together with previously published data from normal subjects. The two groups compared well regarding these selected measurements.

Discussion

In the present study we were able to demonstrate that patients with systemic sclerosis have nondilated hypertrophic left ventricles compared to an age- and sex-matched reference population.

Table 10. Diastolic measures of LV hypertrophy

	Controls n = 38	Patients n = 21	p value
Parasternal short-axis view (papillary level)			
Septum + posterior wall mm	18.6±2.8	23.4±3.6	<0.0005
Wall thickness/cavity ratio	0.39±0.07	0.47±0.09	<0.005
LV myocardial area, cm^2	181.2±31	228.2±54	<0.005
LV myocardial area index cm^2/m^2	998±145	1,325±338	<0.0005
LV mass[1], g	205±37	219±27	NS
LV mass index[1], g/m^2	110±14	134±29	<0.005
Apical four-chamber view			
End-diastolic volume, ml	212±67	170±59	<0.01
End-diastolic volume index ml/m^2	114±30	97±29	<0.05

[1] Plus long-axis measurements, see Methods.

Table 12. Comparison between some variables of the controls and previously published data from normal subjects

	Present study n = 48	Triulzi et al. [10] n = 72
Parasternal long-axis view		
Aortic anulus, mm	2.0 (1.5–2.6)	1.9 (1.4–2.6)
Parasternal short-axis view		
LA anterioposterior S, mm	3.2 (2.0–4.3)	2.9 (2.2–4.1)
Apical four-chamber view		
LA area S, cm^2	13.8 (7.2–20.4)	14.2 (8.8–23.4)
RA area S, cm^2	16.5 (9.5–22.2)	13.5 (8.3–19.5)
LV long-axis D, mm	7.9 (6.1–9.8)	7.8 (6.3–9.5)
LV area D, cm^2	31.4 (18.0–44.8)	33.2 (17.7–47.3)
LV area S, cm^2	20.1 (9.1–31.1)	17.6 (7.9–31.5)
Apical long-axis view		
LV long-axis D, mm	7.7 (6.1–9.3)	8.0 (6.8–9.5)

D = End-diastole; S = end-systole; LA = left atrial; RA = right atrial. Results are means, figures in parentheses indicate ranges.

Table 11. LV systolic function

	Controls n = 38	Patients n = 21	p value
Parasternal short-axis view (papillary plane)			
Fractional area change	0.49±0.14	0.48±0.14	NS
ESWS, 10^3 dyn/cm^2	72±19	60±12	NS
Apical four-chamber view			
Ejection fraction, %	61±9.6	56±10.7	NS
Stroke volume, ml	91±30	68±25	<0.005
Stroke volume index, ml/m^2	48.6±15.5	41.4±17.7	NS

ESWS = End-systolic wall stress.

M mode has been a useful method for the assessment of cardiac function in the last two decades, and reports on standardization of M mode measurements have been published [9]. However, M mode, being a single-beam technique, provides data from only a limited region of the heart. To date there is an abundance of evidence regarding the usefulness of the two-dimensional echocardiography in the evaluation of cardiac performance. The use of modern computer technology in combination with recently published recommendations for quantitation of the left ventricle by two-dimensional echocardiography [11] might provide useful tools for a standardized evaluation of cardiac function [12–14], and it has been suggested that two-dimensional echocardiography gives more accurate measures of LV hypertrophy than M mode [17]. As has been suggested [11], we also used a special mattress with a curved cutout to optimize apical recordings.

In the present study normal subjects were selected from the general population by means of the population register to serve as a standard reference. The measurements obtained from these subjects were concordant with previously published data on normals [10].

Our patients with systemic sclerosis displayed increased wall thickness, wall thickness/cavity ratio and relative LV mass, which is in agreement with our previous findings from M mode echocardiography [5] and the studies by others [3, 18, 19]. Despite LV hypertrophy, the patients proved to have a similar or smaller LV cavity than the matched controls. Increased pulmonary pressure with abnormal configuration of the interventricular septum was not a cause of smaller LV dimensions in our patients since we did not find such septal abnormalities and, furthermore, the right atrial and right ventricular dimensions were not increased in patients indicating essentially normal right-sided pressures. It has been proposed that LV hypertrophy in systemic sclerosis is seen only in the presence of systemic hypertension or increased afterload [20]. The present study, however, shows LV

hypertrophy to exist in the absence of increased afterload. This could be due to the myocardial fibrosis commonly seen in these patients [21], a plausible explanation for the abnormal LV distensibility and early filling properties which we have found in the present study population applying Doppler echocardiography [22].

Ejection phase indices as the fractional area change and ejection fraction were similar in the two groups, which is in accordance with previous M mode echocardiographic findings in the present study population [23]. However, the low stroke volume and tendency to a low end-systolic wall stress also support our previous report indicating mild systolic dysfunction as judged from abnormal systolic time intervals, increased mitral E point to septal separation and a low end-systolic wall stress [23]. As has been described by Douglas et al. [14], we noticed also in the present study population that two-dimensional echocardiography yielded higher end-systolic wall stress values than those calculated from M mode measurements [23].

In conclusion, systemic sclerosis as a cardiac disease carries dimensional aberrations of the left heart. Myocardial fibrosis is a possible etiology of our findings, since patients did not have an increased blood pressure or high prevalence of treated hypertension. Echocardiography is a useful noninvasive method for the detection of cardiac abnormalities in patients with systemic sclerosis. Therefore we consider the recommendation of echocardiography as a routine procedure in systemic sclerosis to be highly pertinent.

Acknowledgements

This study was supported by the Swedish Heart and Lung Foundation, Eris 50-Year Foundation and Josef and Linnea's Carlsson Fund.

References

1 Medsger TA Jr, Masi AT, Rodnan GP, et al: Survival with systemic sclerosis (scleroderma). A life table analysis of clinical and demographic factors in 309 patients. Ann Intern Med 1971;75: 369–376.
2 Orabona ML, Albino O: Systemic progressive sclerosis (or visceral scleroderma). Review of the literature and report of cases. Acta Med Scand 1958;160(suppl 580):163–170.
3 D'Angelo WA, Fries JF, Masi AT, et al: Pathological observations in systemic sclerosis (scleroderma). A study of fifty-eight autopsy cases and fifty-eight matched controls. Am J Med 1969; 46:428–440.
4 Bulkley BH, Klacsmann PG, Hutchins GM: Angina pectoris, myocardial infarction and sudden cardiac death with normal coronary arteries: A clinopathologic study of 9 patients with progressive systemic sclerosis. Am Heart J 1978;95:563–569.
5 Kazzam E, Waldenström A, Landelius J, et al: Non-invasive assessment of diastolic left ventricular function in patients with systemic sclerosis. J Intern Med 1990;228:183–192.
6 Ten Cate FJ, Kloster FE, van Dorf WG, Roelandt J: Dimensions and volumes of left atrium and ventricle determined by single beam echocardiography. Br Heart J 1974;36:737–746.
7 Feigenbaum H: Echocardiography. Philadelphia, Lea & Febiger, 1986.
8 Henry WL, Ware J, Gardin JM, et al: Echocardiography in normal subjects: Growth-related changes that occur between infancy and early adulthood. Circulation 1977;57:278–285.
9 Sahn DJ, DeMaria A, Kisslo J, Weyman AI: The committee on M-mode standardization of the American Society of Echocardiography: Recommendation regarding quantitation in M-mode echocardiography: Results of a survey of echocardiographic measurements. Circulation 1978;58:1072–1078.
10 Triulzi M, Gillam LD, Gentile F, et al: Normal adult cross-sectional echocardiographic values: Linear dimensions and chamber areas. Echocardiography 1984;1:403–426.
11 Schiller N, Shah PM, Crawford M, et al: Recommendations for quantitation of the left ventricle by two-dimensional echocardiography. J Am Soc Echocardiogr 1989;2:358–368.
12 Byrd BF, Finkbeiner W, Bouchard A, et al: Accuracy and reproducibility of clinically acquired two-dimensional echocardiographic mass measurements. Am Heart J 1989;117:133–137.
13 Tortoledo FA, Quinones MA, Fernandez GC, et al: Quantification of left ventricular volumes by two-dimensional echocardiography: A simplified and accurate approach. Circulation 1983; 67:579–584.
14 Douglas PS, Reichek A, Plappert T, et al: Comparison of echocardiographic methods for assessment of left ventricular shortening and wall stress. J Am Coll Cardiol 1987;9:945–951.
15 Subcommittee for scleroderma criteria of American Rheumatism Association, Diagnostic and therapeutic criteria committee: Preliminary criteria for the classification of systemic sclerosis (scleroderma). Arthritis Rheum 1980;23:581–590.
16 Caidahl K, Eriksson H, Wikstrand J, et al: Dyspnea of cardiac origin in 67-year-old men. I. Relation to systolic left ventricular function and wall stress. The study of men born in 1913. Br Heart J 1988;59:319–328.
17 Reichek N, Helak J, Plappert T, et al: Anatomic validation of left ventricular mass estimates from clinical two-dimensional echocardiography: Initial results. Circulation 1983;67:348–352.
18 Bulkley BH, Ridolfi RL, Salyer WR, et al: Myocardial lesions of progressive systemic sclerosis. A cause of cardiac dysfunction. Circulation 1976;53:483–490.
19 Oram S, Stokes W: The heart in scleroderma. Br Heart J 1961; 23:243–259.
20 Follansbee WP: The cardiovascular manifestation of systemic sclerosis (scleroderma). Curr Probl Cardiol 1986;5:242–298.
21 Sackner MA, Heinz ER, Steinberg AJ: The heart in scleroderma. Am J Cardiol 1966;17:542–575.
22 Kazzam E, Caidahl K, Hällgren R, Johansson C, Waldenström A: Mitral regurgitation and diastolic flow profile in systemic sclerosis. Int J Cardiol 1990;29:357–363.
23 Kazzam E, Caidahl K, Gustafsson R, Hällgren R, Landelius J, Waldenström A: Non-invasive assessment of left ventricular systolic function in systemic sclerosis. Eur Heart J 1991;12:151–156.

American Journal of Noninvasive Cardiology
Editor-in-Chief: D.H. Spodick, Worcester, MA

Reprint
Publisher: S. Karger AG, Basel
Printed in Switzerland

Am J Noninvas Cardiol 1991;5:343–352

0258–4425/91/0056–0343$2.75/0

Two-Dimensional Echocardiographic Measurements in Systemic Sclerosis and a Matched Reference Population

Elsadig Kazzam[a], *Kenneth Caidahl*[b], *Tomas Gustafsson*[c], *Rolf Gustavsson*[a], *Roger Hällgren*[a], *Johan Landelius*[d], *Anders Waldenström*[a]

Departments of [a] Internal Medicine and [d] Clinical Physiology, University Hospital, Uppsala;
[b] Department of Clinical Physiology, Sahlgren's University Hospital, and [c] Chalmers School of Technology, Gothenburg, Sweden

Key Words. Cardiac dimensions · Echocardiography · Left atrium · Left ventricle · Systemic sclerosis · Right atrium

Abstract. The present study was performed in order to evaluate, by two-dimensional echocardiography, cardiac morphology in terms of chamber dimensions, as well as left ventricular (LV) volume and mass, in patients with systemic sclerosis (n = 30). Measurements were compared with those from age- and sex-matched controls (n = 48). The most prominent finding in patients was increased LV wall thickness. There was also a tendency in patients to have reduced LV cavity dimensions. Thus, interventricular septum ($p < 0.0005$), LV posterior wall ($p < 0.05$) and the wall thickness/cavity dimension ratio ($p < 0.0005$) were increased in patients compared to controls, as was LV mass index ($p < 0.005$). The stroke volume ($p < 0.005$), end-diastolic volume ($p < 0.01$) as well as end-diastolic volume index ($p < 0.05$) were decreased in the patient group, but not when body surface area was considered. Blood pressure, ejection fraction and end-systolic wall stress were similar in the two groups. We conclude that our patients with systemic sclerosis had a nondilated LV cavity, with an increased wall thickness and relative LV mass. LV hypertrophy was not explained by systemic hypertension and may therefore be secondary to myocardial fibrosis.

Introduction

In systemic sclerosis, cardiac involvement seems to be an indicator of poor prognosis [1, 2]. Postmortem studies [3, 4], and M mode echocardiographic evaluation of the present study population [5], have shown that left ventricular (LV) hypertrophy is a common finding in patients with systemic sclerosis. M mode echocardiography has been extensively used for the noninvasive assessment of cardiac dimensions and performance [6–9], and more recently the usefulness of two-dimensional echocardiographic measurements of cardiac dimensions has been demonstrated [10, 11]. The value of two-dimensional echocardiography in the assessment of LV mass [12], volume [13] and stress [14] has been reported.

The aim of the present study was to evaluate cardiac morphology and LV function by two-dimensional echocardiography in patients with systemic sclerosis in comparison with normal controls.

Patients and Methods

Subjects

Thirty consecutive patients (15 men and 15 females; age range 25–77 years, mean 54.5 years), with systemic sclerosis according to the American Rheumatism Association criteria [15] were studied. The patients were referred from Uppsala region to Uppsala University Hospital between December 1986 and March 1988. Their disease had been recognized for 5.6 (range 0.5–23) years. On electrocardiogram none had left bundle branch block, while 1 patient had

Received: June 10, 1990
Revision received: February 1, 1991
Accepted: February 6, 1991

Address for correspondence:
Dr. Elsadig Kazzam, MD
Department of Internal Medicine, Uppsala University Hospital
S–75 185 Uppsala (Sweden)

Table 1. Clinical data of the individual patients with systemic sclerosis (SScl)

No.	Sex age years	Disease duration years	SScl scoring (0–54)	SBP/ DBP mm Hg	TPR dyn (s cm^{-5})	ESR mm/h	FEV_1 % of predicted	Serum creatinine µmol/l	Medication
1	M 68	12	36	140/73	1,452	85	89	72	–
2	M 54	1	29	95/65	2,284	8	73	79	nifedipine
3	M 68	5	34	125/76	1,714	44	45	107	frusemide
4	M 77	0.5	41	125/77	1,832	36	91	97	–
5	F 43	2	30	132/80	1,191	13	51	85	nifedipine
6	F 48	0.5	34	120/75	593	95	72	90	–
7	F 65	7	27	123/73	1,500	8	93	87	–
8	F 67	23	31	127/70	1,126	95	90	68	–
9	F 66	5	25	130/90	2,085	22	76	59	hydrochlorothiazide
10	F 42	0.5	21	165/80	–	20	100	64	verapamil
11	M 59	20	28	122/61	1,358	20	57	79	–
12	F 65	0.5	16	103/64	1,829	22	66	76	–
13	M 59	3	24	127/79	–	7	80	67	–
14	M 50	0.5	8	138/81	1,275	60	56	71	–
15	M 46	4	21	160/70	1,177	56	91	50	–
16	F 70	8	34	157/110	1,393	20	90	79	–
17	M39	1	11	165/80	1,863	8	75	91	digoxin
18	M 48	1	25	125/75	1,306	7	93	80	–
19	F 73	1	37	133/90	920	4	63	78	–
20	M 27	7	10	125/75	2,123	46	121	110	–
21	M 43	10	31	139/88	1,887	10	109	75	–
22	F 51	1	11	110/73	846	18	66	81	–
23	M 63	5	34	145/77	1,298	67	74	72	–
24	M 66	0.5	34	169/66	1,987	54	71	77	–
25	F 25	0.5	8	105/72	2,238	5	70	76	–
26	F 49	1	25	147/87	1,798	50	67	83	frusemide
27	F 47	10	31	118/77	1,095	–	109	–	–
28	M 67	0.6	19	145/92	1,207	40	67	85	–
29	F 41	–	–	125/68	1,426	34	66	67	–
30	F 48	11	–	158/90	2,569	9	81	65	–

F = Female; M = male; SBP = systolic blood pressure; DBP = diastolic blood pressure; TPR = total peripheral resistance; ESR = erythrocyte sedimentation rate; FEV_1 = forced expiratory volume during 1 s as percentage of predicted.

Table 2. General characteristics of the controls and patients (means ± SD)

	Controls n = 48	Patients n = 30	p value
Age, years	54.9 ± 2.1	54.5 ± 2.4	NS
Sex female/male	26/22	15/15	
Height, cm	172.7 ± 1.1	170.9 ± 1.9	NS
Weight, kg	73.1 ± 1.8	65.1 ± 2.0	< 0.05
BSA, m^2	1.9 ± 0.03	1.7 ± 0.04	< 0.05
Systolic blood pressure mm Hg	134.6 ± 2.6	132.9 ± 3.5	NS
Diastolic blood pressure mm Hg	81.6 ± 1.4	78.7 ± 2.1	NS

right bundle branch block. The clinical characteristics and the status of the individual patients are shown in table 1.

For comparative purposes, age- and sex-matched control subjects were selected from the general population of Uppsala. A sample of 90 age- and sex-matched subjects (3 for each patient) was drawn from the population register kept by the County Census Bureau. All controls were informed about the investigation protocol, and 55 of them gave their consent to participate in the study. Controls were excluded if they were treated for hypertension (n = 2), if they had coronary (n = 2) or rheumatic (n = 2) heart disease according to clinical history or electrocardiogram. None of the controls had known renal or pulmonary disease or bundle branch block. One subject was excluded because of inadequate recordings. The remaining 48 subjects (26 men and 22 females, age range 25–77 years, mean 54.6 years) constituted a healthy control group. The general characteristics of the controls and the patients are shown in table 2.

Methods

Two-dimensional echocardiography was performed by means of a Hewlett Packard ultrasound imaging system model 77020A, version K with a 2.5- or 3.5-MHz phased array transducer. The echocardiographic recordings of routine projections, the parasternal long-axis and short-axis (aortic, mitral and papillary) planes and the apical four-chamber, long-axis and two-chamber views were stored on VHS 0.5-inch video tapes by means of a Panasonic video recorder NV 8100.

One investigator (E.K.) carried out all interpretations, and questionable measuring points were agreed upon by consensus with another investigator (K.C.). For the interpretations a special computer program was developed on a minicomputer (LSI-11/23, Digital Equipment Corp.). A framegrabber with 256-kB image memory (Matrox QVAPH + QRGB, 512*152*8), a digitizer (Graphtec KD6040) and a color monitor (VR241, Digital Equipment Corp.) were used. A videosystem with slow-motion and playback facilities (Panasonic) was connected to the computer through the framegrabber, and the recordings were digitized in real time, interpretation being performed in the digitized form. The matrix consisted of 512 lines, 512 pixels (picture elements)/line and 8 bits of gray scale per pixel. The stop frame mode utilized renewed digitization from the next frame (still frame picture) when the video recorder was stopped.

The end-diastolic and end-systolic frames were localized by using the search feature of the tape recorder. End-diastole was defined as the frame at or immediately preceding the R wave of the QRS complex and (when visualized) after atrioventricular valve closure. End-systole was defined by the aortic valve closure, smallest LV cavity dimension or by an immediately following atrioventricular valve opening, as appropriate, in that order. Measurements were performed by manually tracing borders or marking distances with the digitizer or by moving a cursor through the digitized image on the monitor. Tracings and markings were immediately seen on the monitor, and mistakes could easily be corrected. All measurements were performed using the inner (trailing to leading) edge convention. The mean of three beats was used. However, in recordings with only acceptable general quality, the best beat was used if having a better than average quality. Stop frames were excluded if there was more than 10% drop of the endocardium. Distances were not measured if the endocardium was not visible at both ends of the distance, i.e. measuring points were not interpolated from surrounding echoes. We used only projections where the intended orientation was obtained, i.e. e.g. noncircular short-axis images were excluded from measurements. A concave interventricular septum indicating severe pulmonary hypertension was not found. The analyzed dimensions and areas are described in figure 1.

LV mass was calculated according to the formula $1.05 \cdot \pi\ [(b + t)^2(2/3[a + t] + d - d^3/[3(a + t)^2]) - b^2(2/3 \cdot a + d - d^3/[3 \cdot a^2])]$ [12], where a, b, d and t denote the apical part of the long axis and short axis, the basal part of the long axis and the average wall thickness, respectively. From the LV short-axis view at the level of the papillary muscle the total area (muscular + cavity area; A1) and cavity area (A2) were determined, and the myocardial area (Am) was calculated as Am = A1 – A2. Area fractional shortening and fractional shortening were calculated as (diastolic – systlic)/diastolic cavity area and anterioposterior dimension, respectively. The average wall thickness (t) equals the difference between the radii of epicardial (A1) and endocardial (A2) area: $t = \sqrt{A1/\pi} - \sqrt{A2/\pi}$.

Blood pressure was measured in the supine position after 15–30 min of rest. Carotid pulse tracings were used for calculation of end-systolic pressure, assigning diastolic and systolic blood pressure to the nadir and peak of the curve [16]. Only beats with acceptable or good quality were used for measurements. All measurements of the relative height of end-systole compared to total height of the carotid curve were performed by means of a digitizer-computer system (Summagraphics digitizer connected to a PDP 11/34 computer, Digital Equipment). Five beats were measured from pulse curves. The means were used for further calculations. End-systolic wall stress was obtained as 1.33 × end-systolic pressure × A2/Am × 103 dyn/cm^2 [14].

From the apical four-chamber view the end-diastolic and end-systolic volumes were calculated according to the formula volume = 5/6 × area × LV long axis at end-diastole, and ejection fraction was obtained as end-diastolic – end-systolic/end-diastolic volumes. Stroke volume was calculated as ejection fraction × end-diastolic volume.

Lung function was estimated by the measurement of forced expiratory volume in 1 s, the lower normal value in our laboratory being 80% of the predicted value. The erythrocyte sedimentation rate was read after 1 h (Westergren), and serum creatinine was measured at the Department of Clinical Chemistry.

A Raynaud's phenomenon score was based on a 5-grade scale; 0 for no signs of the phenomenon and 4 for the most severe form with cyanotic fingers even at 20 °C.

The severity of skin lesions was assessed by a simple scoring system; skin thickening was estimated at 18 anatomical sites by a 4-grade scale: 0 for normal skin and grade 3 for the most severe thickening and induration of the skin. The maximum score was therefore 54.

Statistics

Measurements are presented as means ± standard deviation. Student's t test was used to evaluate differences between the study groups.

Results

General Characteristics

The general characteristics of the controls and the patients are shown in table 2. In spite of similar heights, patients weighed less than controls. Blood pressure was similar in the two groups.

Interpretability of Two-Dimensional Echocardiography

In the tables the numbers of controls and patients yielding any stop frame measure in the respective view are specified. It seems also pertinent to present the availability for analyses of relevant structures in the motion mode and the number of investigations allowing all attempted measurements in stop frame mode.

Out of the 30 patients/48 controls the motion mode (and all measures in the stop frame mode) were available

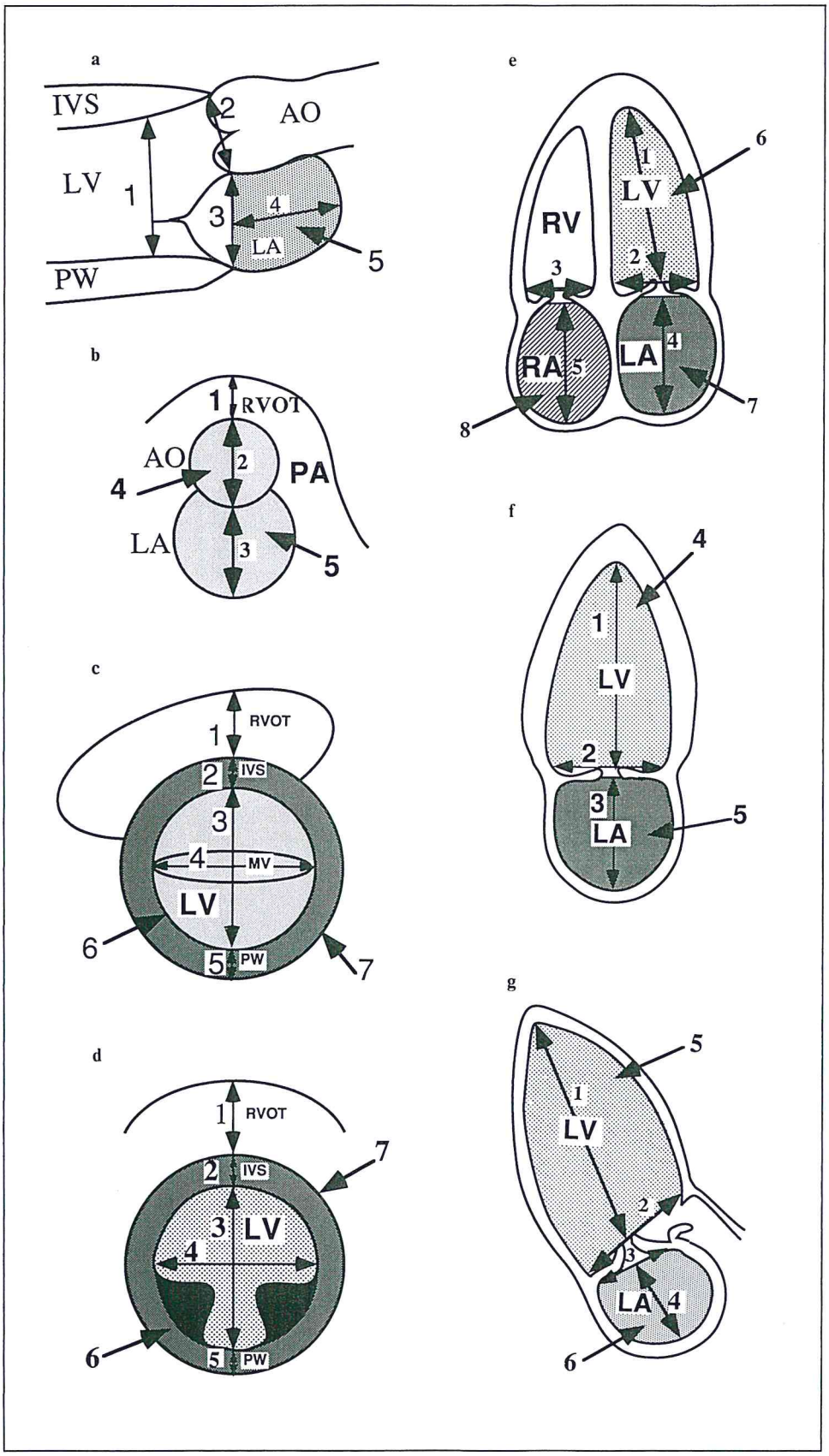

Fig. 1. Measurements of dimensions. In addition to the marked dimensions, the LV area was measured in the apical views, the left atrium in the apical long-axis view and both atria in the four-chamber view. AO = Aorta; IVS = interventricular septum; LA = left atrium; LV = left ventricle; MV = mitral valve; PA = pulmonary artery; PM = papillary muscle; PW = posterior wall; RA = right atrium; RV = right ventricle; RVOT = right ventricular outflow tract.

a Parasternal long-axis view. 1 = LV mid cavity (mitral tip); 2 = AO diameter; 3 = mitral orifice; 4 = LA long-axis diameter; 5 = LA area.

b Parasternal short-axis view: AO level. 1 = RVOT; 2 = AO anterioposterior diameter; 3 = LA anterioposterior diameter; 4 = AO area; 5 = LA urea.

c Parasternal short-axis view: MV level. 1 = RVOT; 2 = septal thickness; 3 = LV anterioposterior diameter; 4 = LV mid cavity diameter; 5 = PW thickness; 6 = LV cavity area; 7 = LV cavity + myocardial area.

d Parasternal short-axis view: PM level. 1 = RVOT; 2 = [illegible]al thickness; 3 = LV anterioposterior diameter; 4 = LV mid cavity diameter; 5 = PW thickness; 6 = LV cavity area; 7 = LV cavity + myocardial area.

e Apical four-chamber view. 1 = LV long axis; 2 = LV base; 3 = RV base; 4 = LA long axis; 5 = RA long axis; 6 = LV area; 7 = LA area; 8 = RA area.

f Apical two-chamber view. 1 = LV long axis; 2 = LV base; 3 = LA long axis; 4 = LV area; 5 = LA area.

g Apical long-axis view. 1 = LV long axis; 2 = LV base; 3 = mitral orifice; 4 = LA long axis; 5 = LV area; 6 = LA area.

Table 3. Left parasternal long-axis view (means ± SD)

		Uncorrected			Adjusted for BSA (/m²)		
		controls n = 43	patients n = 28	p	controls n = 43	patients n = 28	p
Aortic diameter, mm	D	20±2.9	21±3.7	NS	11.1±1.4	12.1±1.8	<0.05
	S	22±3.0	23±3.7	NS	11.8±1.5	13.2±2.2	<0.005
LA mitral orifice, mm	D	23±3.5	25±4.5	NS	12.7±2.0	14.4±2.8	<0.05
	S	33±4.3	34±4.2	NS	18.1±2.4	19.6±3.2	<0.05
LA diameter long-axis, mm	D	31±5.1	35±8.2	<0.05	17.3±2.9	20.4±4.9	<0.005
	S	45±7.1	45±8.3	NS	24.3±4.0	26.5±7.4	NS
LA area, mm²	D	594±184	717±306	<0.05	323±94	416±170	<0.005
	S	1,189±283	1,213±426	NS	647±149	711±282	NS
LV diameter mid cavity, mm	D	47±4.8	48±7.3	NS	25.6±2.8	27.6±4.4	<0.05
	S	35±6.9	36±8.7	NS	19.2±3	20.1±4.6	NS

D = End-diastole; S = end-systole; LA = left atrial; LV = left ventricular.

in the following numbers: parasternal long-axis view 28 (28)/44 (44); parasternal short-axis projection (aortic view) 20 (13)/46 (34); parasternal short-axis (mitral) view 22 (10)/47 (29); parasternal short-axis (papillary) view 22 (11)/46 (28); four-chamber view 27 (23)/47 (46); apical long-axis view 24 (20)/45 (43), and apical two-chamber view 24 (21)/40 (39).

To evaluate the relation between the image quality and age, height, weight, body surface area (BSA) and body mass index, we correlated these variables with picture quality. We found significant correlations between image quality in all views (both motion and stop frame pictures) and age. The quality of apical recordings (motion as well as stop frame) was also significantly correlated to the body mass index.

Dimensions

Dimensional data for each echocardiographic view are presented in tables 3–9. Noncorrected values are shown on the left, and measurements adjusted for BSA are displayed on the right. Since patients had lower BSA than controls, measures having similar values in the uncorrected form gave increased values for patients after adjustment for BSA, while low values among patients turned out to be normal after adjustment for BSA.

The aortic diameter did not differ between patients and controls (tables 3, 4), although after adjustment for BSA patients had a 1 mm larger diameter than controls in the parasternal long-axis view.

The left atrium tended to be larger in patients, but not in all views (tables 3, 4, 7–9). After adjustment for BSA the left atrium was markedly longer, and its systolic area increased in the apical four-chamber view, compared to the left atrium in controls (table 7).

The left ventricle was smaller in patients as judged from apical projections (tables 7–9), but this was not the case when body size was taken into account.

Neither the right atrium (table 7) nor the right ventricle (tables 4–7) were increased among patients. This fact was not influenced by considerations of body size.

The LV myocardial thickness was increased in diastole, whether measured as septal or posterior wall thickness (tables 5, 6). There was a tendency to increased LV wall area, and this measure was clearly abnormal in the parasternal short-axis view at the papillary level when BSA was considered (table 6). Combined measures of LV hypertrophy (table 10) revealed increased LV wall thickness, thickness/cavity ratio as well as LV mass index.

LV Systolic Function

Ejection fraction, fractional area change and end-systolic wall stress were similar in the two groups (table 11). For the patients and controls considered together, calculations of end-systolic wall stress from two-dimensional echocardiography yielded higher values than those previously found from M mode (68.5 ± 2.9 vs. 58.6 ± $1.9 \cdot 10^3$ dyn/cm², $p < 0.005$). Stroke volume was decreased in the patients.

Table 4. Left parasternal short-axis view: aortic level (means ± SD)

		Uncorrected			Adjusted for BSA (/m²)		
		controls n = 43	patients n = 28	p	controls n = 43	patients n = 28	p
Aortic AP diameter, mm	D	25±3.5	25±6.5	NS	14±1.5	14±2.7	NS
	S	29±5.4	29±6.3	NS	15±2.3	16±3.0	NS
Aortic area, mm²	D	489±138	534±223	NS	263±74	298±97	NS
	S	624±178	667±291	NS	335±82	380±128	NS
LAAP diameter, mm	D	26±5.1	28±5.8	NS	14±3.0	16±3.2	NS
	S	32±5.7	33±6.9	NS	17±2.9	19±3.3	NS
LA area, mm²	D	840±333	884±230	NS	456±182	512±146	NS
	S	1,264±348	1,305±400	NS	680±167	750±214	NS
RV outflow tract, mm	D	35±6.3	32±5.9	NS	19±2.7	19±5.8	NS
	S	28±5.8	24±5.5	NS	15±3.0	14±5.1	NS

D = End-diastole; S = end-systole; RV = right ventricular; AP = anterioposterior; LA = left atrial.

Table 5. Left parasternal short-axis view: mitral valve level (means ± SD)

		Uncorrected			Adjusted for BSA (/m²)		
		controls n = 43	patients n = 28	p	controls n = 43	patients n = 28	p
IVS thickness, mm	D	9.8±1.5	12.3±2.2	<0.0005	5.4±0.7	7.1±1.6	<0.0005
	S	12.2±1.7	13.0±2.6	NS	6.7±0.9	7.5±1.9	NS
PW thickness, mm	D	8.4±1.5	10.9±2.0	<0.0005	4.6±0.8	6.4±2.3	<0.0005
	S	11.0±2.3	12.8±3.8	NS	6.1±1.1	7.5±2.9	<0
LV wall area, mm²	D	3,469±743	3,739±846	NS	1,884±325	2,157±581	NS
	S	2,767±527	3,245±717	<0.05	1,515±225	1,864±460	<0.005
LV AP diameter, mm	D	49±5.4	48±7.7	NS	27±2.9	28±4.8	NS
	S	36±5.1	37±9.8	NS	20±2.9	21±6.4	NS
LV mid cavity, mm	D	44±5.6	44±6.4	NS	24±3.2	26±6.9	NS
	S	32±5.7	34±3.4	NS	18±3.4	20±4.2	NS
LV area, mm²	D	1,807±427	17,990±385	NS	988±220	1,023±180	NS
	S	1,115±597	1,079±667	NS	621±372	613±122	NS
RV outflow tract, mm	D	28±11	25±6.8	NS	15±7.3	15±4.4	NS
	S	26±6.1	26±6.5	NS	14±3.1	15±3.6	NS

D = End-diastole; S = end-systole; RV = right ventricular; IVS = interventricular septum; PW = posterior wall; AP = anterioposterior.

Table 6. Left parasternal short-axis view: papillary muscle level (means ± SD)

		Uncorrected			Adjusted for BSA (/m²)		
		controls n = 43	patients n = 28	p	controls n = 43	patients n = 28	p
IVS thickness, mm	D	9.5 ± 1.4	12.6 ± 1.8	< 0.0005	5.2 ± 0.7	7.4 ± 2.1	< 0.0005
	S	12.2 ± 2.4	14.8 ± 3.1	< 0.05	6.7 ± 1.2	8.6 ± 2.3	< 0.0005
PW thickness, mm	D	9.1 ± 1.6	10.7 ± 2.5	< 0.05	5.0 ± 1.0	6.2 ± 2.2	< 0.05
	S	11.2 ± 2.2	14.7 ± 2.9	< 0.0005	6.2 ± 1.2	8.5 ± 2.3	< 0.0005
LV wall area, mm²	D	3,451 ± 461	3,967 ± 561	< 0.05	1,880 ± 193	2,300 ± 461	< 0.0005
	S	2,677 ± 403	3,219 ± 762	< 0.05	1,470 ± 214	1,865 ± 510	< 0.005
LV AP diameter, mm	D	49 ± 4.9	51 ± 6.0	NS	27 ± 2.5	29 ± 5.7	NS
	S	37 ± 9.2	36 ± 6.8	NS	20 ± 6.2	21 ± 4.9	NS
LV mid cavity, mm	D	43 ± 4.9	43 ± 4.9	NS	24 ± 3.0	25 ± 7.2	NS
	S	28.7 ± 4.8	30.8 ± 4.4	NS	16 ± 2.8	18 ± 5.0	NS
LV area, mm²	D	1,707 ± 288	1,781 ± 305	NS	931 ± 144	1,021 ± 199	NS
	S	855 ± 217	928 ± 280	NS	472 ± 133	531 ± 163	NS
RV outflow tract, mm	D	23 ± 6.2	21 ± 6.8	NS	13 ± 3.1	12 ± 6.2	NS
	S	26 ± 6.1	26 ± 7.1	NS	14 ± 3.2	14 ± 5.7	NS

D = End-diastole; S = end-systole; RV = right ventricular; IVS = interventricular septum; PW = posterior wall.

Table 7. Apical four-chamber view (means ± SD)

		Uncorrected			Adjusted for BSA (/m²)		
		controls n = 43	patients n = 28	p	controls n = 43	patients n = 28	p
LA long-axis diameter, mm	D	37 ± 7.0	44 ± 9.9	< 0.01	20 ± 3.6	25 ± 5.4	< 0.0005
	S	49 ± 6.8	52 ± 8.2	NS	27 ± 4.2	30 ± 4.9	< 0.005
LA area, mm²	D	933 ± 801	1,068 ± 329	NS	513 ± 501	620 ± 199	NS
	S	1,382 ± 330	1,580 ± 384	< 0.05	613 ± 214	748 ± 167	< 0.005
RA long-axis diameter, mm	D	40 ± 7.3	42 ± 8.7	NS	22 ± 3.8	24 ± 4.7	< 0.05
	S	50 ± 5.8	51 ± 7.8	NS	27 ± 3.4	30 ± 4.7	< 0.05
RA area, mm²	D	1,141 ± 306	1,241 ± 388	NS	615 ± 159	719 ± 213	< 0.05
	S	1,652 ± 334	1,664 ± 390	NS	892 ± 171	967 ± 207	NS
LV long-axis diameter, mm	D	80 ± 9.2	73 ± 9.6	< 0.01	43 ± 4.7	43 ± 5.0	NS
	S	66 ± 9.9	63 ± 9.2	NS	36 ± 4.6	36 ± 4.9	NS
LV base diameter, mm	D	44 ± 5.1	44 ± 6.1	NS	24 ± 2.5	25 ± 3.2	< 0.05
	S	36 ± 6.2	35 ± 7.9	NS	20 ± 3.1	20 ± 4.0	NS
LV area, mm²	D	3,140 ± 668	2,720 ± 596	< 0.05	1,960 ± 268	1,566 ± 289	NS
	S	2,010 ± 551	1,713 ± 469	< 0.05	1,079 ± 251	982 ± 235	NS
RV base diameter, mm	D	38 ± 4.6	36 ± 7.0	NS	21 ± 2.7	21 ± 3.5	NS
	S	31 ± 4.2	31 ± 5.8	NS	17 ± 2.4	18 ± 2.8	NS

D = End-diastole; S = end-systole; RV = right ventricular; RA = right atrial; LA = left atrial.

Table 8. Apical long-axis view (means ± SD)

		Uncorrected			Adjusted for BSA (/m²)		
		controls n = 43	patients n = 28	p	controls n = 43	patients n = 28	p
LA mitral orifice, mm	D	27±3.8	26±4.8	NS	14±1.8	15±3.3	NS
	S	32±6.1	31±5.2	NS	17±3.2	18±3.2	NS
LA long-axis diameter, mm	D	43±7.0	46±9.9	NS	24±4.3	27±6.0	<0.05
	S	55±6.2	54±7.7	NS	30±4.5	32±6.0	NS
LA area, mm²	D	890±253	1,007±340	NS	481±126	587±186	<0.05
	S	1,516±335	1,650±464	NS	821±174	961±266	<0.05
LV long-axis diameter, mm	D	75±9.7	71±9.8	NS	41±5.3	42±5.3	NS
	S	62±9.7	60±8.1	NS	34±5.0	36±5.9	NS
LV base diameter, mm	D	46±5.3	44±6.6	NS	25±2.6	26±4.4	NS
	S	37±6.6	36±10	NS	20±3.3	21±6.4	NS
LV area, mm²	D	2,831±511	2,425±604	<0.05	1,529±244	1,415±288	NS
	S	1,835±501	1,454±414	<0.005	989±245	853±232	<0.05

D = End-diastole; S = end-systole; RV = right ventricular; RA = right atrial; LA = left atrial.

Table 9. Apical two-chamber view (means ± SD)

		Uncorrected			Adjusted for BSA (/m²)		
		controls n = 43	patients n = 28	p	controls n = 43	patients n = 28	p
long-axis diameter, mm	D	43±8.3	42±8.4	NS	23±4.7	25±5.8	NS
	S	55±8.3	51±8.6	NS	30±5.0	31±607	NS
LA area, mm²	D	1,116±262	1,234±387	NS	600±155	739±250	<0.0
	S	1,784±319	1,753±396	NS	958±185	1,056±311	NS
LV long-axis diameter, mm	D	77±8.3	71±8.9	<0.05	41±5.1	43±8.4	NS
	S	64±9.1	60±8.2	NS	35±5.3	36±7.1	NS
LV base diameter, mm	D	45±5.2	41±7.5	<0.05	24±3.0	25±6.4	NS
	S	35±6.1	30±6.1	<0.005	19±3.6	18±3.9	NS
LV area, mm²	D	2,934±541	2,398±431	<0.0005	1,568±262	1,444±355	NS
	S	1,818±493	1,479±417	<0.05	971±243	880±242	NS

D = End-diastole; S = end-systole; LA = left atrial.

Control Group Compared to Previously Published Data from Normals

In table 12 some measurements from the controls are displayed together with previously published data from normal subjects. The two groups compared well regarding these selected measurements.

Discussion

In the present study we were able to demonstrate that patients with systemic sclerosis have nondilated hypertrophic left ventricles compared to an age- and sex-matched reference population.

Table 10. Diastolic measures of LV hypertrophy

	Controls n = 38	Patients n = 21	p value
Parasternal short-axis view (papillary level)			
Septum + posterior wall mm	18.6 ± 2.8	23.4 ± 3.6	< 0.0005
Wall thickness/cavity ratio	0.39 ± 0.07	0.47 ± 0.09	< 0.005
LV myocardial area, cm^2	181.2 ± 31	228.2 ± 54	< 0.005
LV myocardial area index cm^2/m^2	998 ± 145	1,325 ± 338	< 0.0005
LV mass[1], g	205 ± 37	219 ± 27	NS
LV mass index[1], g/m^2	110 ± 14	134 ± 29	< 0.005
Apical four-chamber view			
End-diastolic volume, ml	212 ± 67	170 ± 59	< 0.01
End-diastolic volume index ml/m^2	114 ± 30	97 ± 29	< 0.05

[1] Plus long-axis measurements, see Methods.

Table 12. Comparison between some variables of the controls and previously published data from normal subjects

	Present study n = 48	Triulzi et al. [10] n = 72
Parasternal long-axis view		
Aortic anulus, mm	2.0 (1.5–2.6)	1.9 (1.4–2.6)
Parasternal short-axis view		
LA anterioposterior S, mm	3.2 (2.0–4.3)	2.9 (2.2–4.1)
Apical four-chamber view		
LA area S, cm^2	13.8 (7.2–20.4)	14.2 (8.8–23.4)
RA area S, cm^2	16.5 (9.5–22.2)	13.5 (8.3–19.5)
LV long-axis D, mm	7.9 (6.1–9.8)	7.8 (6.3–9.5)
LV area D, cm^2	31.4 (18.0–44.8)	33.2 (17.7–47.3)
LV area S, cm^2	20.1 (9.1–31.1)	17.6 (7.9–31.5)
Apical long-axis view		
LV long-axis D, mm	7.7 (6.1–9.3)	8.0 (6.8–9.5)

D = End-diastole; S = end-systole; LA = left atrial; RA = right atrial. Results are means, figures in parentheses indicate ranges.

Table 11. LV systolic function

	Controls n = 38	Patients n = 21	p value
Parasternal short-axis view (papillary plane)			
Fractional area change	0.49 ± 0.14	0.48 ± 0.14	NS
ESWS, 10^3 dyn/cm^2	72 ± 19	60 ± 12	NS
Apical four-chamber view			
Ejection fraction, %	61 ± 9.6	56 ± 10.7	NS
Stroke volume, ml	91 ± 30	68 ± 25	< 0.005
Stroke volume index, ml/m^2	48.6 ± 15.5	41.4 ± 17.7	NS

ESWS = End-systolic wall stress.

M mode has been a useful method for the assessment of cardiac function in the last two decades, and reports on standardization of M mode measurements have been published [9]. However, M mode, being a single-beam technique, provides data from only a limited region of the heart. To date there is an abundance of evidence regarding the usefulness of the two-dimensional echocardiography in the evaluation of cardiac performance. The use of modern computer technology in combination with recently published recommendations for quantitation of the left ventricle by two-dimensional echocardiography [11] might provide useful tools for a standardized evaluation of cardiac function [12–14], and it has been suggested that two-dimensional echocardiography gives more accurate measures of LV hypertrophy than M mode [17]. As has been suggested [11], we also used a special mattress with a curved cutout to optimize apical recordings.

In the present study normal subjects were selected from the general population by means of the population register to serve as a standard reference. The measurements obtained from these subjects were concordant with previously published data on normals [10].

Our patients with systemic sclerosis displayed increased wall thickness, wall thickness/cavity ratio and relative LV mass, which is in agreement with our previous findings from M mode echocardiography [5] and the studies by others [3, 18, 19]. Despite LV hypertrophy, the patients proved to have a similar or smaller LV cavity than the matched controls. Increased pulmonary pressure with abnormal configuration of the interventricular septum was not a cause of smaller LV dimensions in our patients since we did not find such septal abnormalities and, furthermore, the right atrial and right ventricular dimensions were not increased in patients indicating essentially normal right-sided pressures. It has been proposed that LV hypertrophy in systemic sclerosis is seen only in the presence of systemic hypertension or increased afterload [20]. The present study, however, shows LV

hypertrophy to exist in the absence of increased afterload. This could be due to the myocardial fibrosis commonly seen in these patients [21], a plausible explanation for the abnormal LV distensibility and early filling properties which we have found in the present study population applying Doppler echocardiography [22].

Ejection phase indices as the fractional area change and ejection fraction were similar in the two groups, which is in accordance with previous M mode echocardiographic findings in the present study population [23]. However, the low stroke volume and tendency to a low end-systolic wall stress also support our previous report indicating mild systolic dysfunction as judged from abnormal systolic time intervals, increased mitral E point to septal separation and a low end-systolic wall stress [23]. As has been described by Douglas et al. [14], we noticed also in the present study population that two-dimensional echocardiography yielded higher end-systolic wall stress values than those calculated from M mode measurements [23].

In conclusion, systemic sclerosis as a cardiac disease carries dimensional aberrations of the left heart. Myocardial fibrosis is a possible etiology of our findings, since patients did not have an increased blood pressure or high prevalence of treated hypertension. Echocardiography is a useful noninvasive method for the detection of cardiac abnormalities in patients with systemic sclerosis. Therefore we consider the recommendation of echocardiography as a routine procedure in systemic sclerosis to be highly pertinent.

Acknowledgements

This study was supported by the Swedish Heart and Lung Foundation, Eris 50-Year Foundation and Josef and Linnea's Carlsson Fund.

References

1 Medsger TA Jr, Masi AT, Rodnan GP, et al: Survival with systemic sclerosis (scleroderma). A life table analysis of clinical and demographic factors in 309 patients. Ann Intern Med 1971;75: 369–376.
2 Orabona ML, Albino O: Systemic progressive sclerosis (or visceral scleroderma). Review of the literature and report of cases. Acta Med Scand 1958;160(suppl 580):163–170.
3 D'Angelo WA, Fries JF, Masi AT, et al: Pathological observations in systemic sclerosis (scleroderma). A study of fifty-eight autopsy cases and fifty-eight matched controls. Am J Med 1969; 46:428–440.
4 Bulkley BH, Klacsmann PG, Hutchins GM: Angina pectoris, myocardial infarction and sudden cardiac death with normal coronary arteries: A clinopathologic study of 9 patients with progressive systemic sclerosis. Am Heart J 1978;95:563–569.
5 Kazzam E, Waldenström A, Landelius J, et al: Non-invasive assessment of diastolic left ventricular function in patients with systemic sclerosis. J Intern Med 1990;228:183–192.
6 Ten Cate FJ, Kloster FE, van Dorf WG, Roelandt J: Dimensions and volumes of left atrium and ventricle determined by single beam echocardiography. Br Heart J 1974;36:737–746.
7 Feigenbaum H: Echocardiography. Philadelphia, Lea & Febiger, 1986.
8 Henry WL, Ware J, Gardin JM, et al: Echocardiography in normal subjects: Growth-related changes that occur between infancy and early adulthood. Circulation 1977;57:278–285.
9 Sahn DJ, DeMaria A, Kisslo J, Weyman AI: The committee on M-mode standardization of the American Society of Echocardiography: Recommendation regarding quantitation in M-mode echocardiography: Results of a survey of echocardiographic measurements. Circulation 1978;58:1072–1078.
10 Triulzi M, Gillam LD, Gentile F, et al: Normal adult cross-sectional echocardiographic values: Linear dimensions and chamber areas. Echocardiography 1984;1:403–426.
11 Schiller N, Shah PM, Crawford M, et al: Recommendations for quantitation of the left ventricle by two-dimensional echocardiography. J Am Soc Echocardiogr 1989;2:358–368.
12 Byrd BF, Finkbeiner W, Bouchard A, et al: Accuracy and reproducibility of clinically acquired two-dimensional echocardiographic mass measurements. Am Heart J 1989;117:133–137.
13 Tortoledo FA, Quinones MA, Fernandez GC, et al: Quantification of left ventricular volumes by two-dimensional echocardiography: A simplified and accurate approach. Circulation 1983; 67:579–584.
14 Douglas PS, Reichek A, Plappert T, et al: Comparison of echocardiographic methods for assessment of left ventricular shortening and wall stress. J Am Coll Cardiol 1987;9:945–951.
15 Subcommittee for scleroderma criteria of American Rheumatism Association, Diagnostic and therapeutic criteria committee: Preliminary criteria for the classification of systemic sclerosis (scleroderma). Arthritis Rheum 1980;23:581–590.
16 Caidahl K, Eriksson H, Wikstrand J, et al: Dyspnea of cardiac origin in 67-year-old men. I. Relation to systolic left ventricular function and wall stress. The study of men born in 1913. Br Heart J 1988;59:319–328.
17 Reichek N, Helak J, Plappert T, et al: Anatomic validation of left ventricular mass estimates from clinical two-dimensional echocardiography: Initial results. Circulation 1983;67:348–352.
18 Bulkley BH, Ridolfi RL, Salyer WR, et al: Myocardial lesions of progressive systemic sclerosis. A cause of cardiac dysfunction. Circulation 1976;53:483–490.
19 Oram S, Stokes W: The heart in scleroderma. Br Heart J 1961; 23:243–259.
20 Follansbee WP: The cardiovascular manifestation of systemic sclerosis (scleroderma). Curr Probl Cardiol 1986;5:242–298.
21 Sackner MA, Heinz ER, Steinberg AJ: The heart in scleroderma. Am J Cardiol 1966;17:542–575.
22 Kazzam E, Caidahl K, Hällgren R, Johansson C, Waldenström A: Mitral regurgitation and diastolic flow profile in systemic sclerosis. Int J Cardiol 1990;29:357–363.
23 Kazzam E, Caidahl K, Gustafsson R, Hällgren R, Landelius J, Waldenström A: Non-invasive assessment of left ventricular systolic function in systemic sclerosis. Eur Heart J 1991;12:151–156.